Stabilized Polymers with Novel Indenoindene Backbone against Photodegradation for LEDs and Solar Cells

Suhee Song,[†] Youngeup Jin,*[,†] Sun Hee Kim,[‡] Jihyun Moon,[†] Kwanghyun Kim,[§] Jin Young Kim,[‡,||] Sung Heum Park,[‡,||] Kwanghee Lee,*[,‡] and Hongsuk Suh*[,†]

Department of Chemistry and Chemistry Institute for Functional Materials, Pusan National University, Busan 609-735, Korea, LG Electronics Incorporated, Kumi, Kyungbuk, 730-030, Korea, Department of Materials Science and Engineering Gwangju Institute of Science and Technology, Gwangju 500-712, Korea, and Center for Polymers and Organic Solids, University of California at Santa Barbara, Santa Barbara, California 93106-5096

Received June 25, 2008; Revised Manuscript Received August 6, 2008

ABSTRACT: PPV derivatives, polymers with vinylene units, have their tendency to exhibit degradation, after irradiation with white light or operation of the device, resulting in the appearance of a shifted absorption and emission band in the short wavelength regions of the spectra. In this paper, we report the synthesis and properties of new polymers utilizing new backbone, poly(5,5,10,10-tetrakis(2-ethylhexyl)-5,10-dihydroindeno[2,1-*a*]indene-2,7-diyl) (PININE). In order to reduce oxidation of the vinylene group, the vinylene group was cyclized using two 5-membered rings. While poly(*p*-phenylenevinylene) derivatives show significantly blue-shifted and decreased peaks of UV−vis, blue-shifted maximum peaks of photoluminescence (PL) after irradiation with white light in air, and blue-shifted maximum peaks of electroluminescence (EL) after operation of the device, PININE shows stable spectra of UV−vis, and PL, and EL under the same conditions. PININE copolymers with benzothiadiazole and thiophene units exhibit high power conversion efficiency (PCE) for polymer solar cells. Under white light illumination (AM 1.5 G, 100 mW/cm^2), the cell based on PININEDTBT/PCBM as the active layer has a short circuit current density (I_{sc}) of 5.93 mA/cm^2, a fill factor (FF) of 43%, and PCE of 1.88%. These copolymers have not only good processability due to the indenoindene unit, in which four alkyl groups can be incorporated, but also strong and uniform absorbance in the whole visible region.

1. Introduction

Since polymeric light-emitting diodes (PLEDs) based on poly(*p*-phenylenevinylene) (PPV)[1,2] were reported, various kinds of conjugated polymers have been developed for electroluminescence (EL) and solar cells.[3−5] PPVs with vinylene units, including DP-PPV[6] for green, "Super Yellow",[7,8] for yellow, and CN-PPV[9,10] for red, have acquired much attention because of their high luminescence and fluorescence quantum yields.[11] Along with extensive research of conjugated polymers, stabilized blue color polymers, poly(fluorene) (PF)[12,13] and poly(cyclopenta[*def*]phenanthrene) (PCPP)[14,15] etc., which do not contain vinylene units, have been utilized for the main backbone.[16,17] The most representative configuration of polymer solar cells is bulk heterojunction device which is composed of a blend of an electron-donating material (p-type), and an electron-accepting material (n-type) such as (6,6)-phenyl C_{61}-butyric acid methyl ester (PCBM). Many new conjugated polymers with a small band gap are being researched for polymer solar cells (PSCs), since red shift of the absorption spectrum indeed helps increase the total photovoltaic current.[18,19]

"Super Yellow", which is a PPV derivative, is still being used to produce the highest efficiency. By the way, one problem associated with these PPV derivatives with vinylene units is their tendency to exhibit degradation, after irradiation with white light or operation of the device, resulting in the appearance of a shifted absorption and emission band in the short wavelength regions of the spectra and a concomitant drop of EL quantum efficiency.[20,21] Photo-oxidation of the vinylene group of the PPVs can introduce carbonyl groups,[22−24] which are efficient PL quenchers at the termina of the polymer chains to cause the reduction of luminescence yield.[25] Excited-state singlet oxygen appears to be responsible for the photo-oxidation via [2 + 2] cycloaddition between singlet oxygen and the vinylene double bond.[26] Since the photo-oxidation results in chain scission with consequent reduction of the conjugation length of the polymer, absorption and emission bands are shifted to blue.[27] As compared to the case of stilbene monomer compound, the extended conjugation length of the polymers, in this case PPVs, increases the electron density at the double bond, which gives rise to the higher reactivity to the singlet oxygen electrophile. It was also reported that the presence of electron-rich groups on the phenylene rings in PPV derivatives increases the likelihood of photo-oxidation.[28] To improve the stability of the vinylene units of PPVs, there have been several reports including incorporation of electron-withdrawing groups on the π-system,[29] or utilization of efficient singlet oxygen quencher.[28] Although it has already been reported that a cyclized vinylene group in a stilbene derivative can prohibit *cis*−*trans* isomerization,[30] there has been no report about the inhibition of photodegradation using a cyclized vinylene group. The structure of the repeating unit in poly(5,5,10,10-tetrakis(2-ethylhexyl)-5,10-dihydroindeno[2,1-*a*]indene-2,7-diyl) (PININE) can prevent the oxidation of the vinylene units. As shown in Chart 1, in the case of PPV derivatives, 1,2-diphenylethene unit A will be oxidized to dicarbonyl compound C, via dioxetane B.[24] The conversion from dioxetane B to dicarbonyl compound C is facile due to the increase of entropy. However, in the case of PININE, oxidation of dihydroindenoindene unit D, which can lead to diketone F upon reaction with singlet oxygen, is almost impossible, as compared to the case of PPV derivatives. Dihydroindenoindene unit D cannot be oxidized to diketone F, via dioxetanes E, since the first and second steps are reversible[31] and D is more stable than F.

* Corresponding authors. E-mail: hssuh@pusan.ac.kr; klee@gist.ac.kr; yej@pusan.ac.kr.
[†] Pusan National University.
[‡] Gwangju Institute of Science and Technology.
[§] LG Electronics Incorporated.
[||] University of California at Santa Barbara.

10.1021/ma801420e CCC: $40.75
Published on Web 09/27/2008

Chart 1. Mechanism of the Degradations of the Polymers

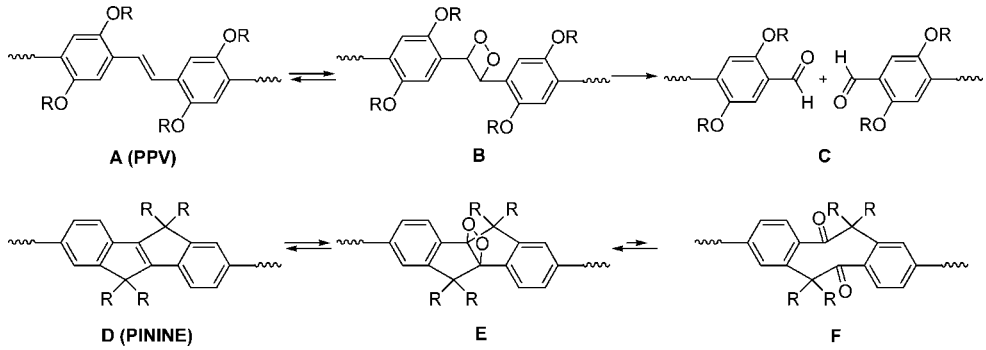

Scheme 1. Synthetic Route for the Synthesis of the Monomer and PININE

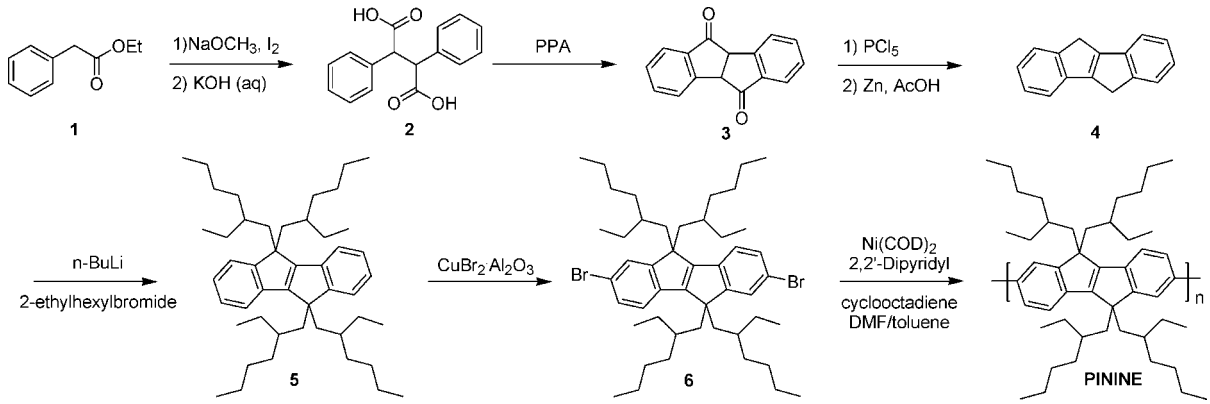

After poly(3-hexylthiophene) (P3HT)[32−35] with absorption covering only a part of the visible light had been investigated to further improve the absorption properties of the conjugated polymers, some narrow band gap polymers, including thiophene[36−39] and benzothiadiazole (BT),[40] were synthesized and applied to the PSCs.[32−35,41−44] Even though BT is one of the best moieties to induce the narrow band gap since its structure causes low solubility, its copolymers with other units which can improve the processability have been investigated extensively. Since polyfluorenes and their derivatives have the advantage of good solubility in common organic solvents,[20,45,46] emission color can be changed over an entire visible region by introducing narrow band gap comonomers into the polyfluorene backbone. The low energy level of the HOMO of PFs can increase the V_{oc} of its copolymers. For this reason, the syntheses and properties of low band gap polymers derived from fluorene and sulfur-containing heterocyclic materials were reported. Since polyfluorene homopolymers have large band gaps, it was not really easy to reduce the band gaps of the copolymers for application in photovoltaic devices.[47]

In this paper, we report the synthesis and properties of new polymers for EL and solar cells utilizing a new backbone, PININE, poly(2,7-dihydroindeno[2,1-*a*]indene-*co*-2,1,3-benzothiadiazole) (PININEBT), poly(2,7-dihydroindeno[2,1-*a*]indene-*co*-4,7-di-2-thienyl-2,1,3-benzothiadiazole) (PININEDTBT), poly(2,7-dihydroindeno[2,1-*a*]indene-*co*-4,7-bis(4-hexyl-2-thienyl)-2,1,3-benzothiadiazole)(PININEDHTBT), and poly(2,7-dihydroindeno[2,1-*a*]indene-*co*-4,7-bis[3-(hexyloxy)-2-thienyl]-2,1,3-benzothiadiazole) (PININEDHOTBT). In order to reduce oxidation of the vinylene group, the vinylene group was cyclized using two 5-membered rings. The polymer, PININE, contains stilbene chromophore, but the vinylene group is located in the bicyclic [2.2.0] system. In the case of PININE, it is possible to introduce four alkyl groups to the sp^3 carbons in the bicycle, which will increase the solubility of the polymer, without distorting the conjugation, to be applied as an efficient electroluminescence layer for the light-emitting diodes (LEDs). Since the copolymers including indenoindene and BT units have stable backbone, high solubility and low band gap, they can be utilized as efficient electron-donating materials with large V_{oc} for the photovoltaic devices.

2. Results and Discussion

2.1. Synthesis and Characterization. The general synthetic routes toward the monomers and polymers are outlined in Schemes 1 and 2. In the first step, ethyl phenylacetate (**1**) was converted to 2,3-diphenylsuccinic acid (**2**) using I_2 and KOH.[48] The cyclization of resulting dicarboxylic acid **2** was achieved with polyphosphoric acid to give 4b,9b-dihydroindeno[2,1-*a*]indene-5,10-dione (**3**).[49] Dione **3** was treated with PCl_5 in $CHCl_3$ followed by Zn and acetic acid to generate indeno[2,1-*a*]indene **4**. Alkylation of indeno[2,1-*a*]indene **4** with ethylhexyl bromide and *n*-BuLi in hexane afforded 5,5,10,10-tetrakis(2-ethylhexyl)-5,10-dihydroindeno[2,1-*a*]indene (**5**). Compound **5** was brominated in carbon tetrachloride by alumina-supported copper(II) bromide to give monomer 2,7-dibromo-5,5,10,10-tetrakis(2-ethylhexyl)-5,10-dihydroindeno[2,1-*a*]indene (**6**) with high selectivity. Using Yamamoto coupling conditions,[50] the PININE was synthesized using $Ni(COD)_2$, cyclooctadiene and bipyridyl in toluene and DMF (dimethyl formamide). Bis(pinacolato)diboron was reacted with dibromo compound **6** using catalytic amounts of $Pd(dppf)Cl_2$, and potassium acetate in DMF to provide 4,4,5,5-tetramethyl-2-[5,5,10,10-tetrakis(2-ethylhexyl)-7-(4,4,5,5-tetramethyl-1,3,2-dioxaborolan-2-yl)-4b,5,9b,10-tetrahydroindeno[2,1-*a*]inden-2-y]-1,3,2-dioxaborolane (**7**). Monomer **7** was copolymerized with monomers **8**−**11** by using the palladium-catalyzed Suzuki coupling method.[51] The yields of the resulting polymers were over 45%. All the polymers exhibited excellent solubility in common organic solvents such

Scheme 2. Synthetic Route for the Synthesis of PININE Copolymers

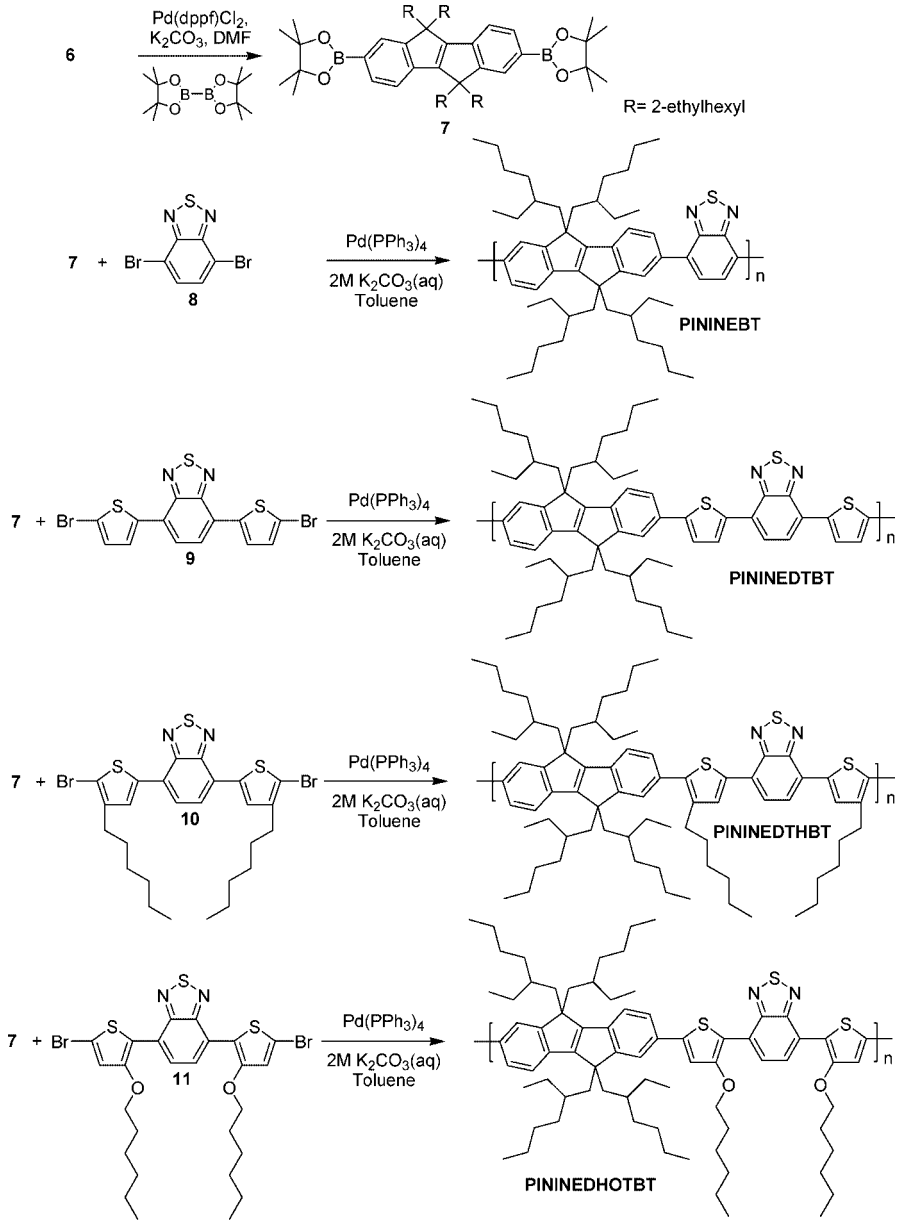

Table 1. Polymerization Results and Thermal Properties of Polymers

polymer	yield (%)	M_n[a]	M_w[a]	PDI[a]	DSC (T_g)	TGA (T_d)[b]
PININE	62	95000	304000	3.2	104	375
PININEBT	60	28000	46000	1.6	107	381
PININEDTBT	45	38000	70000	1.8	108	361
PININEDHTBT	60	17000	28000	1.6	106	351
PININEDHOTBT	67	26000	44000	1.6	88	348

[a] Molecular weight (M_w) and polydispersity (PDI) of the polymers were determined by gel permeation chromatography (GPC) in THF using polystyrene standards. [b] Onset decomposition temperature (5% weight loss) measured by TGA under N_2.

as chloroform, tetrahydrofuran, dichloromethane, and chlorobenzene. Molecular weights and polydispersities of the polymers were determined by gel permeation chromatography (GPC) analysis with a polystyrene standard calibration. Table 1 summarized the polymerization results including molecular weights, PDI and thermal stability of the polymers. The number-average molecular weight (M_n) of 17,000−95,000 and weight-average molecular weight (M_w) of 28,000−304,000 with PDI (poly dispersity index, M_w/M_n) of 1.6−3.2 of the resulting polymers were determined by GPC. The molecular weight of PININE synthesized by Yamamoto coupling was higher than that of other copolymers with Suzuki coupling.

2.2. Thermal Properties. The thermal properties of the polymers were characterized by both differential scanning calorimetry (DSC) and thermal gravimetric analysis (TGA). The differential scanning calorimetry analysis was performed under a nitrogen atmosphere (50 mL/min) on a DSC 822 at heating rates of 10 °C/min. Thermal gravimetric analysis was performed with a Dupont 951 TGA instrument in a nitrogen atmosphere at a heating rate of 10 °C/min to 800 °C. The polymers show good thermal stability with high glass transition temperatures (T_g) of 88−108 °C and onset decomposition temperatures (T_d, 5% weight loss) of 348−381 °C under nitrogen. The high thermal stability of the resulting polymers prevents the deformation of the polymer morphology and the degradation of the polymeric emitting layer by applied electric fields of LEDs.

2.3. Optical and Photoluminescence Properties. The optical and photoluminescence properties of the polymer were investigated both in chloroform solution and in thin film. The

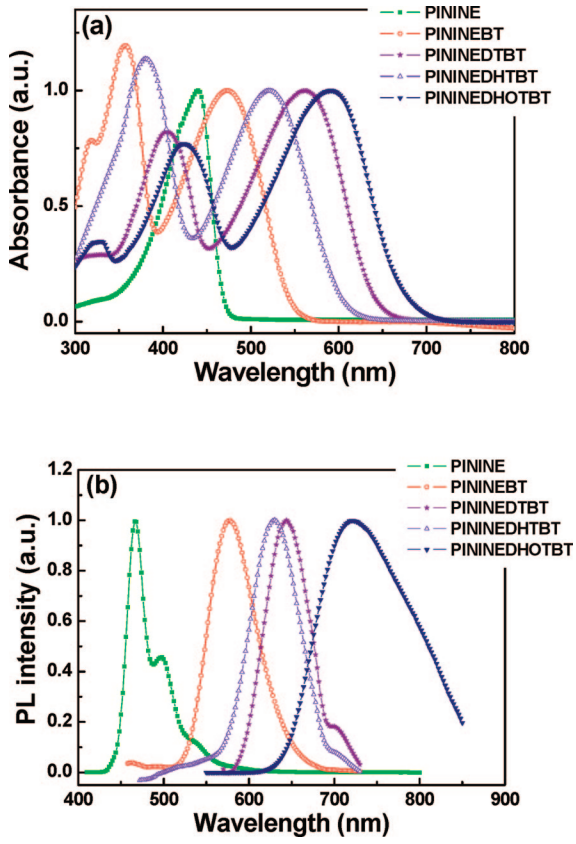

Figure 1. UV−visible absorption (a) and PL (b) spectra of polymer in chloroform solution.

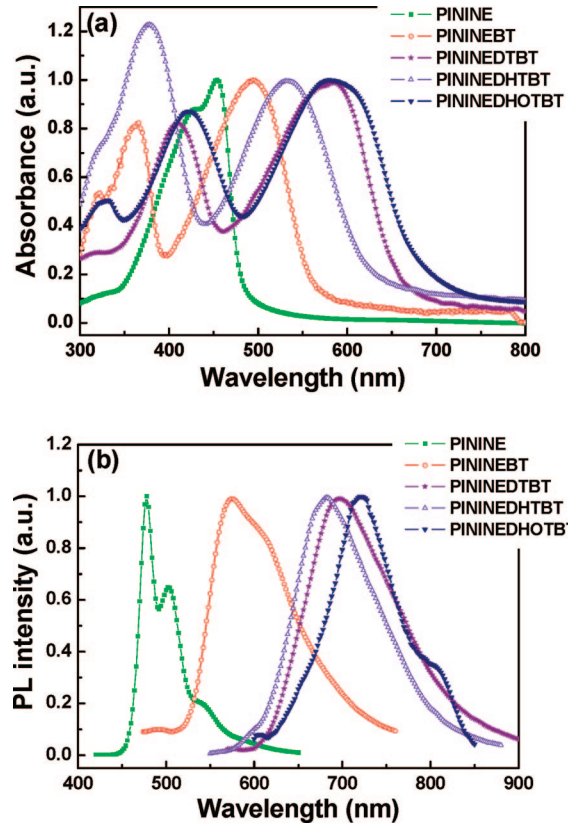

Figure 2. UV−visable absorption (a) and PL (b) spectra of polymer in the solid state.

absorption and emission data for the polymers are shown in Figures 1 and 2 and summarized in Table 2. The concentration of the chloroform solution of the polymer was fixed at 1×10^{-5} M. Transparent and uniform polymer film was prepared on quartz plates by spin-casting from their chlorobenzene solution at room temperature. The absorption spectrum of PININE exhibited a maximum peak at 440 nm in solution of chloroform and at 454 nm in thin film. The PL spectrum of the polymer in solution shows typical vibronically structured bands comprising a maximum and a shoulder, which appear at 467 and 497nm. In the case of thin film, the PL spectrum showed a maximum at 478 nm and a shoulder at 503 nm. Both the absorption and the emission spectra of the film are red-shifted as compared to the case of the solution state, probably because of the increased intermolecular interactions. The absolute PL quantum efficiency (Φ_{PL}) of the PININE in solution and thin film was measured in an integrating sphere at room temperature in air to be 82.5% and 11.6%, respectively. The PL spectrum of PININE was blue-shifted as compared to those of PPV derivatives, and red-shifted as compared to those of poly(*p*-phenylene) (PPPs) or PFs. Even though there is a fused vinylene unit in the repeating units, PININE shows a blue-shifted PL spectrum as compared to the case of PPVs, since there is no vinylene group between the repeating units. PININE showed a red-shifted PL spectrum as compared to the case of PPPs or PFs, which was caused by the increased effective conjugation length due to the cyclized vinylene group in the repeating units.

The absorption spectrum of PININEBT exhibited maximum peaks at 360 and 473 nm in solution of chloroform and at 360 and 494 nm in thin film. According to the BT unit incorporated, two distinct absorption bands were observed both in the solution and in the solid states. The maximum peak of PININEBT was red-shifted by 33−40 nm more than PININE and the absorption band at 360 nm was formed due to the $\pi-\pi^*$ transition mainly occurring in the monomeric units. The PL spectrum of the polymer shows a maximum peak at 575 nm with solution and thin film, and was red-shifted with about 100 nm as compared to PININE. The color was changed to orange, which was more red-shifted than the case of PF−BT copolymer since PININE has a longer effective conjugation length than PF.

Table 2. Characteristics of the UV-vis Absorption, Photoluminescence, and Electroluminescence Spectra

	in solution		in thin film		
polymer	abs λ_{max} (nm)	PL λ_{max} (nm)	abs λ_{max} (nm)	PL λ_{max} (nm)	EL λ_{max} (nm)
PININE	440	467	454	478	477
PININEBT	473	575	494	575	570
PININEDTBT	565	650	580	700	665
PININEDHTBT	520	630	530	685	650
PININEDHOTBT	605	720	605	720	

In the case of copolymers with indenoindene, BT and thiophene, which are PININEDTBT, PININEDHTBT and PININEDHOTBT, the spectra of UV absorption and PL emission were more red-shifted than PININEBT. The absorption spectra of the polymers exhibited maximum peaks at 375−415 nm and 520−605 nm in solution of chloroform and at 375−415 nm and 530−605 nm in thin film. The PL spectra of the polymers show maximum peaks at 630−720 nm with solution and 685−720 nm with thin film. Both the absorption and the emission spectra in thin film are red-shifted as compared to the case of the solution state, probably because of the increased intermolecular interactions due to electron withdrawing BT units and rigid thiophene backbone.

Photodegradation experiments were performed by illuminating the thin film with white light from a halogen lamp (300 W, 110 V GE), placed at 25 cm distance from the sample. The optical properties of MEH-PPV and PININE after irradiation of the thin films up to 60 min were evaluated. As shown in

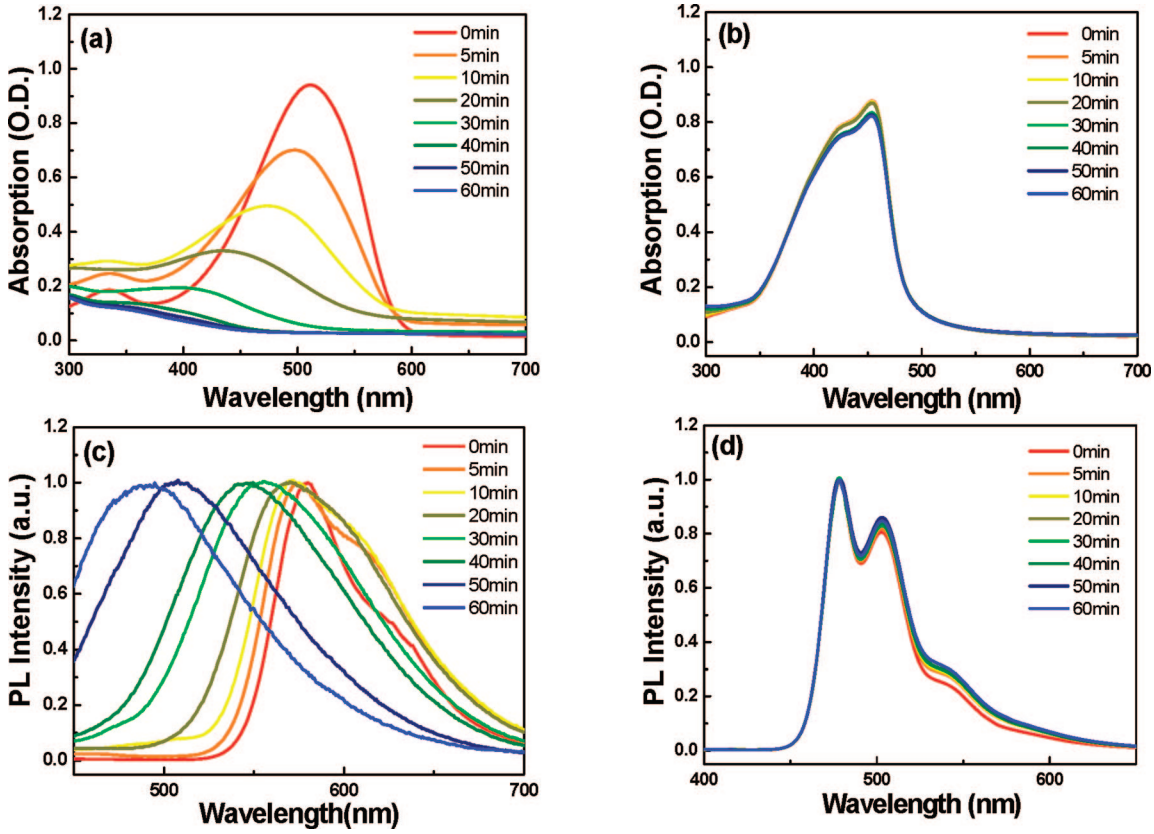

Figure 3. Absorption spectra of (a) MEH-PPV and (b) PININE after different exposure times with white light in air. PL spectra of (c) MEH-PPV and (d) PININE after different exposure times with white light in air. The excitation wavelength was 400 nm. PL spectra are normalized to show blue shift.

Figure 3(a), the photo-oxidation of MEH-PPV led to remarkable changes in the UV−vis spectra. As irradiation time increases, absorption maxima of MEH-PPV are blue-shifted. Moreover, the optical density of absorption spectrum is decreased as the exposure time increases. After 40 min of irradiation, the absorption maximum peak has disappeared. This phenomenon results from the loss of the vinylene group, therefore reducing the conjugation length of the polymer and causing the photobleaching of the polymer. However, in the case of UV−vis spectra of PININE, there is almost no decrease of the optical density. In addition to this, the maximum peak was observed at the same wavelength all through the irradiation period as shown in Figure 3(b). Figure 3 (c) and (d) shows PL spectra of PININE with increasing irradiation time. In case of MEH-PPV, the maximum peak at 580 nm is blue-shifted significantly to show the maximum peak at 492 nm after irradiation for 60 min. The CIE coordinates of PL spectra of MEH-PPV were significantly changed from (0.55, 0.43) to (0.19, 0.14). As shown in the Supporting Information, other PPV derivatives, including poly(2-dimethyloctylsilyl-1,4-phenylenevinylene) (Si-PPV) and poly(9,9-di-*n*-octylfluorenyl-2,7-vinylene) (PFV), also exhibit similar phenomena, which indicates severing the vinylene group to cause the reduction of the conjugation length of the polymer. In the case of PININE, the maximum peak was constantly at 478 nm and the Commission Internationale de L'Eclairage[52] (CIE) coordinates were only very slightly changed from (0.16, 0.33) to (0.17, 0.35). PL spectra of PININE are very stable as compared with PPV derivatives, because the oxidation of the polymer is protected due to the bicyclic [2.2.0] system.

2.4. Electrochemical Properties. The electrochemical properties of the polymer were determined from the band gaps which were estimated from the absorption edges, and the HOMO energy levels which were estimated from the cyclic voltammetry (CV). The absorption onset wavelength of PININE was observed

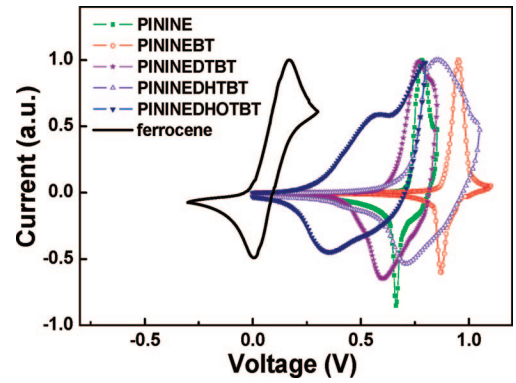

Figure 4. Electrochemical properties of PININE derivatives.

at 500 nm in solid thin film, which corresponds to a band gap of 2.48 eV. The absorption onset wavelengths of alternating polymers in thin film were at 693−570 nm, which corresponds to band gaps of 1.79−2.18 eV. The CV was performed with a solution of tetrabutylammonium tetrafluoroborate (Bu_4NBF_4) (0.10 M) in acetonitrile at a scan rate of 100 mV/s at room temperature. A platinum electrode (~0.05 cm^2) coated with a thin polymer film was used as the working electrode. Pt wire and a $Ag/AgNO_3$ electrode were used as the counter and reference electrode, respectively. The energy level of the $Ag/AgNO_3$ reference electrode (calibrated by the Fc/Fc^+ redox system) was 4.8 eV below the vacuum level. The cyclic voltammograms are shown in Figure 4, and the oxidation onsets are summarized in Table 3. HOMO levels were calculated according to the empirical formula ($E_{HOMO} = -([E_{onset}]^{ox} + 4.8)$ eV). The polymers exhibit irreversible processes in an oxidation scan. The oxidation onsets of polymers were estimated to be 0.32−0.80 V, which correspond to HOMO energy levels

Table 3. Electrochemical Potentials and Energy Levels of the Copolymers

polymers	E_{onset}[a] (V)	HOMO[b] (eV)	LUMO[c] (eV)	E_g[d] (eV)
PININE	0.72	−5.52	−3.04	2.48
PININEBT	0.80	−5.60	−3.42	2.18
PININEDTBT	0.65	−5.45	−3.61	1.84
PININEDHTBT	0.72	−5.52	−3.56	1.96
PININEDHOTBT	0.32	−5.12	−3.33	1.79

[a] Onset oxidation potential measured by cyclic voltammetry. [b] Calculated from the oxidation potentials. [c] Calculated from the HOMO energy levels and E_g. [d] Energy band gap was estimated from the onset wavelength of the optical absorption.

of −5.12 to −5.60 eV. Since the reduction waves were hardly obtained, the LUMO energy levels of polymers were calculated with the HOMO energy levels and optical band gaps. The LUMO energy levels of polymers were thus determined to be −3.04 to −3.61 eV.

2.5. Electroluminescent Properties and Current Density−Voltage−Luminescence (*J*−*V*−*L*) Characteristics. The electroluminescence performance of the polymers was examined in the device configuration of ITO/PEDOT:PSS/polymer/Ba:Al. The EL spectra of the polymers were nearly the same as the PL of the polymers, indicating that the EL and PL phenomena originated from the same excited state. The EL spectrum of PININE exhibited a maximum peak at 478 nm, which corresponds to sky-blue. In the case of alternating polymers, EL emission spectra showed dominant peaks by the BT unit and thiophene backbone at around 570−665 nm.

The change of the EL spectra after operation of the ITO/PEDOT:PSS/polymer/Al device is shown in Figure 5 and Table 4. In order to investigate the influence of the electrical field on polymer degradation, two identical devices with MEH-PPV and PININE were electrically stressed for 1, 10, 40, 80, and 120 min under nitrogen environment. In the case of MEH-PPV, the maximum peak of electroluminescence spectra is blue-shifted to 563 nm, which is a similar phenomenon with that from the photo-oxidation although the degradation rate by electrical stress was lower than that of photo-oxidation. However, in the case of PININE, the initial maximum peak of the EL spectrum was cleanly preserved even after operation of the device for up to 120 min in nitrogen atmosphere. Even though the peak around 540 nm, possibly caused by the aggregation, was slightly increased before 10 min, the whole EL spectrum was not changing at all and showed exactly the same CIE coordinates of (0.20, 0.36) after operation of the device over 10 min up to 120 min. In the case of PININEBT, the EL spectra showed a maximum peak at 570 nm, and the EL emission color remained orange and stable over the operating voltage range of the diode without variation of the CIE coordinates as shown in Figure 6. The EL spectra of the alternating copolymers with BT and thiophene units showed the range of deep red and near IR, and these copolymers could be expected to be utilized as low band gap materials for photovoltaic cells while the EL efficiencies were very low.

The current density−voltage−luminescence (*J*−*V*−*L*) characteristics and efficiencies of the devices with the configuration of ITO/PEDOT:PSS/PININE or PININEBT/Ba:Al are shown in Figure 7. The voltage−current density characteristics of the devices fabricated from PININE and PININEBT reveal that the turn-on voltages are 6.5 and 6 V (Table 5). The maximum brightness of PININE is 2187 cd/m^2 at 12 V, and the maximum luminescence efficiency is 0.34 cd/A at 162 mA/cm^2. In the case of PININEBT, the maximum brightness is 797 cd/m^2 at 10 V, and the maximum luminescence efficiency is 0.23 cd/A at 213 mA/cm^2.

2.6. Polymer Photovoltaic Properties. The current−voltage characteristics of the solar cells, under simulated 100 mW/cm^2 AM 1.5 G white light illumination, based on the three blends PININEDTBT/PCBM, PININEDHTBT/PCBM, and PININEDHOTBT/PCBM are shown in Figure 8, and Table 6 lists the photovoltaic properties obtained from the *J*−*V* curves for the best devices. The PSCs had a layered structure of glass/ITO/PEDOT:PSS/polymer−PCBM blend/Al where the polymer was used as the electron donor and PCBM was used as the electron acceptor. The solar cell made from copolymer PININEDTBT exhibits high power conversion efficiency (PCE). PININEDTBT has not only good processability due to PININE backbone, in which four alkyl groups can be incorporated, but also low HOMO value (−5.45 eV). Generally, V_{oc} is a measure of the difference between the oxidation potential of the donor (PININEDTBT, PININEDHTBT and PININEDHOTBT) and the reduction potential of the acceptor (PCBM).[46,53] The low HOMO level of PININEDTBT accounts for the high V_{oc} value

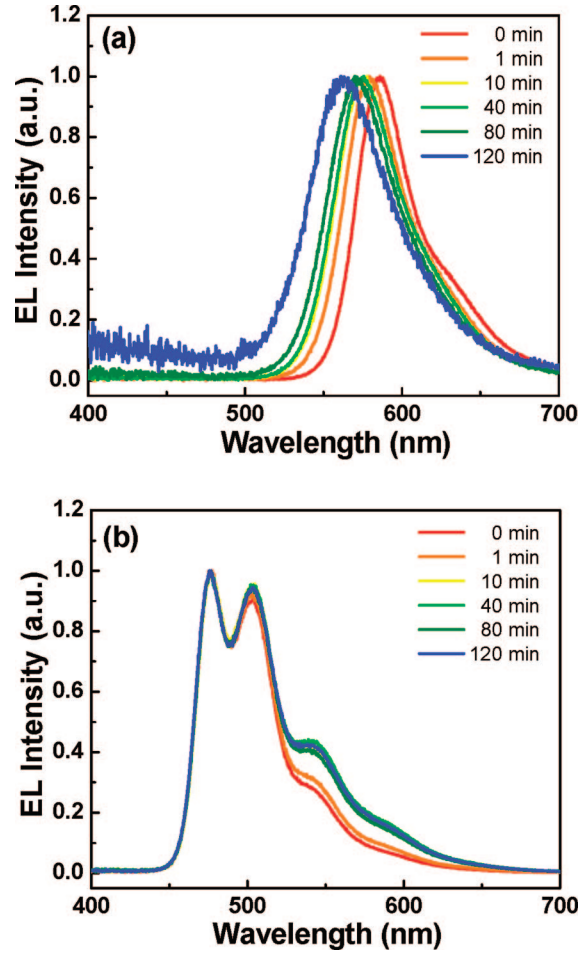

Figure 5. EL spectra of (a) MEH-PPv and (b) PININE on operation of the ITO(150 nm)/PEDOT(10 nm)/polymer(30 nm)/Al(150 nm) device at the different operating times in nitrogen atmosphere. Data are shown for elapsed time of device operation of 0, 1, 10, 40, 80, and 120 min.

Table 4. EL Spectral Data and CIE Coordinates of the Devices of MEH-PPV and PININE

	MEH-PPV		PININE	
time (min)	EL λ_{max} (nm)	CIE (x, y)[a]	EL λ_{max} (nm)	CIE (x, y)[a]
0	587	(0.55, 0.43)	478, 503	(0.16, 0.32)
1	579	(0.55, 0.45)	478, 503	(0.17, 0.33)
10	575	(0.51, 0.44)	478, 503	(0.20, 0.36)
40	574	(0.51, 0.48)	478, 503	(0.20, 0.36)
80	569	(0.42, 0.48)	478, 503	(0.20, 0.36)
120	563	(0.37, 0.45)	478, 503	(0.20, 0.36)

[a] Calculated from the EL spectrum.

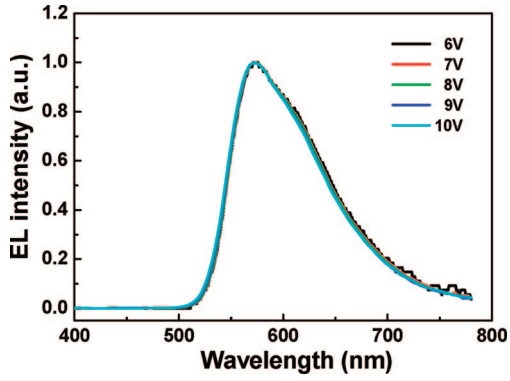

Figure 6. Color stability of devices with the configuration of ITO/PEDOT/PININEBT/Ca/Al at various voltage.

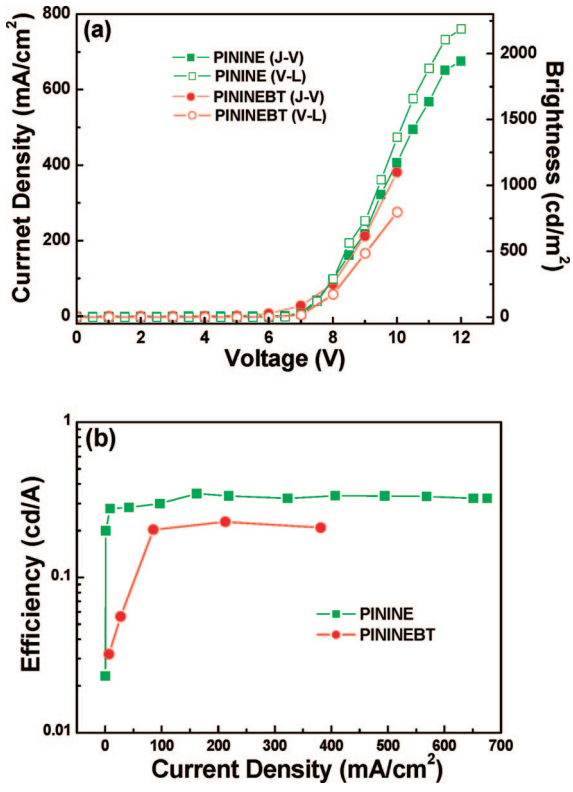

Figure 7. Current−voltage−luminescence ($J-V-L$) characteristics (a) and efficiency (b) of OLEDs with configuration of ITO/PEDOT:PSS/PININE and PININEBT/Ba:Al.

Table 5. Device Performance Characteristics of PCPPBTs

feed ratio of copolymers	turn-on voltage[a] (V)	voltage[b] (V)	current density[b] (mA/cm²)	luminance[b] (cd/m²)	LE_{max}[c] (cd/A)	CIE (x, y)[d]
PININE	6.5	12	675	2187	0.34	(0.17, 0.33)
PININEBT	6	10	381	798	0.23	(0.54, 0.46)
PININEDTBT	4	6	2954	116	0.004	(0.69, 0.31)
PININEDHTBT	3	5	1066	43	0.004	(0.65, 0.34)

[a] Voltages required to achieve a brightness of 1 cd/m². [b] Measured under the condition of maximum brightness. [c] Maximum luminescence efficiency. [d] Calculated from the EL spectrum.

of 0.74 V. Alkyl and alkoxy groups were introduced into the thiophene unit to induce the change of HOMO levels of PININEDHTBT and PININEDHOTBT.

The weight ratio of PININEDTBT to PCBM has a significant influence on the performance of the cell. As shown in the Supporting Information, after examination of several ratios, it was found that the best performance is from the blend with the weight ratio of 1:3.5 to generate a short circuit current density

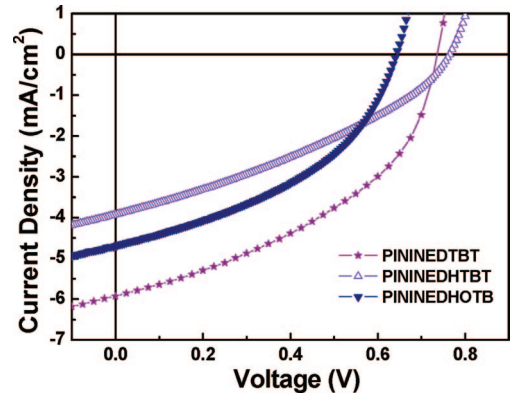

Figure 8. $J-V$ curves of the polymer solar cells based on PININEDTBT, PININEDHTBT, and PININEDHOTBT under the illumination of AM 1.5, 100 mW/cm².

Table 6. Photovoltaic Properties of the Polymer Solar Cells

polymers	V_{OC} (V)	J_{SC} (mA/cm²)	FF	PCE (%)
PININEDTBT	0.74	5.93	0.43	1.88
PININEDHTBT	0.77	3.93	0.34	1.03
PININEDHOTBT	0.64	4.69	0.43	1.28

(J_{sc}) of 5.93 mA/cm², a fill factor (FF) of 43%, and a power conversion efficiency of 1.88%. The raising HOMO of PININEDHOTBT substituted with alkoxy group, which have electron donating effect, diminished the value of V_{oc} due to more closing with LUMO of PCBM. In the case of PININEDHTBT with alkyl group, even though V_{oc} was increased as compared to PININEDTBT caused by the decreased HOMO level, J_{sc} and FF are diminished due to low mobility or interface morphology caused by steric hindrance. Under the same white light illumination, for PININEDHTBT/PCBM and PININEDHOTBT/PCBM, J_{sc} values are 3.93 and 4.69 mA/cm², V_{oc} values are 0.77 and 0.64 V, FF values are 34 and 43%, and PCEs are 1.03 and 1.28%, respectively.

Figure 9 shows the incident photon to concerted current efficiency (IPCE) of the PSCs for the best device as a function of wavelength, which follows the copolymer's UV−vis absorption spectrum, indicating that all the absorption of the polymers contributed to the photovoltaic conversion. The strong and uniform absorbance of the conjugated polymers in the whole visible region increased the total photovoltaic current because a high efficiency polymer photovoltaic material has a higher solar photon flux in this energy range. The integral area of the absorbance of PININEDTBT and PININEDHOTBT in the visible region is higher than that of PININEDHTBT, and the PCEs of the device based on PININEDTBT and PININEDHOTBT

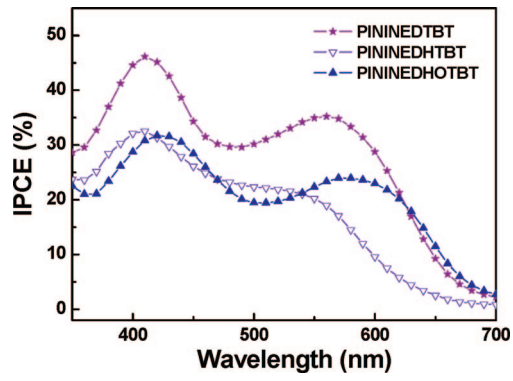

Figure 9. IPCE curves of the polymer solar cells based on PININEDTBT, PININEDHTBT, and PININEDHOTBT under the illumination of AM 1.5, 100 mW/cm².

are also higher than that of PININEDHTBT due to the stronger absorbance in the longer wavelength range from 550 to 650 nm. The motivation of the design and synthesis of the conjugated PININE with BT and thiophene is the production of new conjugated polymers for application in polymer solar cells (PSCs). The unique structure incorporated in the polymers, with great stability against photodegradation and high efficiency even with basic PSC device structure, will be able to be introduced in many more applications in polymeric solar cells as promising materials.

3. Conclusions

In this paper, we report the synthesis and properties of new conducting polymers, PININE, PININEBT, PININEDTBT, PININEDHTBT and PININEDHOTBT. In order to reduce oxidation of the vinylene group, the vinylene group was cyclized using two carbon-containing 5-membered rings. It is possible to introduce four alkyl groups in the sp^3 carbons in the bicycle, which will increase the solubility of the polymer. For the polymerizations to generate PININE derivatives, Yamamoto condition with Ni(0) catalysis and palladium-catalyzed Suzuki coupling were employed. PININE and PININEBT, with good solubility in common organic solvents and good thermal stability, were used as the electroluminescence layer for the LEDs (ITO/PEDOT:PSS/polymer/Ba:Al), and PININEDTBT, PININEDHTBT and PININEDHOTBT were used as the electron donor for the PSCs (ITO/PEDOT:PSS/polymer:PCBM/Al). While PPV derivatives show significantly blue-shifted and decreased peaks of UV−vis and blue-shifted maximum peaks of PL and EL, PININE shows stable spectra of UV−vis, and PL after irradiation with white light in air and EL after operation of the device. The unique structure of PININE, incorporating the vinylene unit with bicyclic [2.2.0] system, can overcome the basic degradation problem of the common type of vinylene units in PPV series. The solar cells made from conjugated PININEs with BT and thiophene units, which are new conjugated polymers for application in polymer solar cells (PSCs), exhibit high PCEs even in basic PSC device structure. These polymers have not only good processability due to the PININE backbone, in which four alkyl groups can be incorporated, but also strong and uniform absorbance in the whole visible region. Polymers with this unique backbone will be able to be introduced in many more applications in polymeric solar cells as promising materials.

4. Experimental Section

General. All reagents were purchased from Aldrich or TCI, and used without further purification. Solvents were purified by normal procedure and handled under moisture-free atmosphere. ^{1}H and ^{13}C NMR spectra were recorded with a Varian Gemini-300 (300 MHz) spectrometer, and chemical shifts were recorded in ppm units with TMS as the internal standard. Flash column chromatography was performed with Merck silica gel 60 (particle size 230−400 mesh ASTM) with ethyl acetate/hexane or methanol/methylene chloride gradients unless otherwise indicated. Analytical thin layer chromatography (TLC) was conducted using Merck 0.25 mm silica gel 60F precoated aluminum plates with fluorescent indicator UV254. High resolution mass spectra (HRMS) were recorded on a JEOL JMS-700 mass spectrometer under electron impact (EI) or fast atom bombardment (FAB) conditions in the Korea Basic Science Institute. Elemental analyses (EA) were performed by Flash EA 1112 series. Molecular weight and polydispersity of the polymer were determined by gel permeation chromatography (GPC) analysis with a polystyrene standard calibration. The UV−vis absorption spectra were recorded by a Varian 5E UV/vis/NIR spectrophotometer, while the Oriel InstaSpec IV CCD detection system with xenon lamp was used for the photoluminescence and electroluminescence spectra measurements. For the EL experiment, poly(3,4-ethylenedioxythiophene) (PEDOT) doped with poly(styrenesulfonate) (PSS), as the hole-injection-transport layer, was introduced between emissive layer and ITO glass substrate cleaned by successive ultrasonic treatments. The solution of the PEDOT:PSS in aqueous isopropyl alcohol was spin-coated on the surface-treated ITO substrate and dried on a hot plate for 30 min at 110 °C. On top of the PEDOT:PSS layer, the emissive polymer film was obtained by spin casting chlorobenzene solution of the polymer. The emissive polymer thin film prepared had a uniform surface with a thickness of around 110 nm. The emissive film was dried in vacuum, and aluminum electrodes were deposited on the top of the polymer films through a mask by vacuum evaporation at pressures below 10^{-7} Torr, yielding active areas of 4 mm^2. For the determination of device characteristics, current density−voltage ($J-V$) and luminance−voltage ($L-V$) characteristics of the devices were measured using a Keithley 236 Source Measure Unit equipped with a calibrated photomultiplier tube. For the color stability experiments, thin films using PININE and MEH-PPV were illuminated with white light from a halogen lamp for 60 min in air, and devices were also operated for 120 min in N_2.

Synthesis of 2,3-Diphenylsuccinic Acid (2). To a stirred solution of sodium methoxide (6.56 g, 121.8) in THF (140 mL) was added ethyl phenylacetate (**1**) (20.0 mL, 121.8 mmol) at −78 °C under argon. The reaction mixture was treated with iodine (15.5 g, 60.9 mmol) in THF (75 mL) over 10 min. After 30 min at room temperature, the reaction mixture was treated with 5% aqueous sodium bisulfate solution (25 mL). To the reaction mixture was added potassium hydroxide (25.3 g, 450.6 mmol) in water (375 mL). After stirring at 40 °C for 5 h, the reaction mixture was treated with 20 mL of concentrated hydrochloric acid. After cooling the reaction mixture, the precipitate was filtered, washed with 20 mL of water, and dried under reduced pressure at room temperature for 24 h to give 15.97 g (49%) of 2,3-diphenylsuccinic acid (**2**) as a white powder: mp 252 °C; R_f 0.28 (SiO_2, methanol:methylene chloride = 1:49); ^{1}H NMR (300 MHz, acetone-d_6, δ) 4.34 (s, 2H), 7.46 (m, 6H), 7.50 (d, 4H, J = 1.6 Hz); ^{13}C NMR (75 MHz, acetone-d_6, δ) δ (ppm) 54.99, 128.27, 129.01, 129.19, 138.05, 173.12; HRMS (EI$^+$, m/z) [M]$^+$ calcd for $C_{16}H_{15}O_4$ 271.0970, found 271.0970. Anal. Calcd for $C_{16}H_{15}O_4$: C 71.10, H 5.22, O 23.68. Found: C 70.64, H 4.83, O 23.19.

Synthesis of 4b,9b-Dihydroindeno[2,1-*a*]indene-5,10-dione (3). To a stirred solution of polyphosphoric acid (500 mL) at 100 °C was added 2,3-diphenylsuccinic acid (**2**) (6.0 g, 22.2 mmol). The reaction mixture was heated at 125−130 °C under argon for 21 h, and then at 150 °C for 2 h. The reaction mixture was cooled to 80 °C, poured into water (600 mL), stirred for 2 h, and filtered. The precipitate was treated with hot 5% sodium bicarbonate aqueous solution (140 mL), stirred for 30 min, and filtered. The precipitate was dried under reduced pressure at 80 °C for 12 h to give 4.5 g (86%) of 9,10-dioxosuccindane **3** as a white solid: mp 205 °C; R_f 0.16 (SiO_2, ethyl acetate:hexane = 1:6); ^{1}H NMR (300 MHz, $CDCl_3$, δ) 4.43 (s, 2H), 7.46 (t, J = 7.5 Hz, 2H), 7.70 (t, J = 7.7 Hz, 2H), 7.73 (d, J = 7.0 Hz, 2H), 7.94 (d, J = 7.6 Hz, 2H); ^{13}C NMR (75 MHz, $CDCl_3$, δ) 52.42, 124.62, 126.42, 128.98, 134.72, 135.73, 149.67, 201.49; HRMS (EI$^+$, m/z) [M]$^+$ calcd for $C_{16}H_{10}O_2$ 234.0681, found 234.0685. Anal. Calcd for $C_{16}H_{10}O_2$: C 82.04, H 4.30, O 13.66. Found: C 81.60, H 4.23, O 13.58.

Synthesis of 5,10-Dihydroindeno[2,1-*a*]indene (4). To a stirred solution of 4b,9b-dihydroindeno[2,1-*a*]indene-5,10-dione (**3**) (14.0 g, 59.8 mmol) in chloroform (50 mL) at room temperature under argon was added phosphorus pentachloride (26.1 g, 125.5 mmol). The flask, fitted with a reflux condenser and gas outlet, was heated in a water bath up to about 50 °C. The reaction was so vigorous that it was necessary to cool the reaction mixture in an ice bath. After refluxing the solution for 30 min, the resulting solution was concentrated under reduced pressure. The mixture was diluted with boiling acetic acid (250 mL), and treated slowly with zinc dust (75 g). The suspension was filtered hot, and the precipitate was washed with boiling acetic acid. The combined filtrate was concentrated under reduced pressure, and purified by flash chromatography to give 13.1 g (91%) of 5,10-dihydroindeno[2,1-*a*]indene (**4**) as a white

solid: mp 209 °C; R_f 0.25 (SiO_2, 100% hexane); ^{1}H NMR (300 MHz, $CDCl_3$, δ) 3.65 (s, 4H), 7.22 (t of d, J = 7.4 and 1.4 Hz, 2H), 7.33 (d of t, J = 7.4 and 1.1 Hz, 2H), 7.45 (d of t, J = 7.4 and 1.1 Hz, 2H), 7.53 (d, J = 7.4 Hz, 2H); ^{13}C NMR (75 MHz, $CDCl_3$, δ) 32.70, 119.15, 124.42, 124.73, 126.61, 141.37, 147.22, 150.77; HRMS (EI$^+$, m/z) [M]$^+$ calcd for $C_{16}H_{12}$ 204.0939, found 204.0938. Anal. Calcd for $C_{16}H_{12}$: C 94.08, H 5.92. Found: C 93.78, H 5.71.

Synthesis of 5,5,10,10-Tetrakis(2-ethylhexyl)-5,10-dihydroindeno[2,1-*a*]indene (5). To a stirred solution of 5,10-dihydroindeno[2,1-*a*]indene (**4**) (1.9 g, 9.3 mmol) in THF (10 mL) at −78 °C under argon was slowly added *n*-BuLi (1.60 M in hexane) (34.8 mL, 55.8 mmol). After 10 min at −78 °C, the reaction mixture was treated with 2-ethylhexyl bromide (7.8 mL, 55.8 mmol). The reaction mixture was stirred for 3 h at room temperature, and treated with 1 N aqueous HCl solution (4 mL). The organic phase was isolated and the aqueous phase was extracted with methylene chloride (2 × 100 mL). The combined organic extract was dried with $MgSO_4$, concentrated under reduced pressure, and purified by flash chromatography to give 3.3 g (64%) of compound **5** as a colorless oil: R_f 0.90 (SiO_2, 100% hexane); ^{1}H NMR (300 MHz, $CDCl_3$, δ) 0.48−1.31 (m, 60H), 1.99 (s, 8H), 7.09 (t, J = 7.4 Hz, 2H), 7.20 (t, J = 7.4 Hz, 2H), 7.31 (d, J = 7.4 Hz, 2H), 7.35 (d, J = 7.4 Hz, 2H); ^{13}C NMR (75 MHz, $CDCl_3$, δ) 10.18, 13.98, 22.85, 26.82, 28.09, 34.05, 34.57, 42.57, 53.81, 119.77, 123.23, 123.63, 126.19, 140.65, 155.57, 155.63; HRMS (FAB$^+$, m/z) [M]$^+$ calcd for $C_{48}H_{76}$ 652.5947, found 652.5948. Anal. Calcd for $C_{48}H_{76}$: C 88.27, H 11.73. Found: C 88.46, H 11.41.

Synthesis of 2,7-Dibromo-5,5,10,10-tetrakis(2-ethylhexyl)-5,10-dihydroindeno[2,1-*a*]indene (6). To a stirred solution of 5,5,10,10-tetrakis(2-ethylhexyl)-5,10-dihydroindeno[2,1-*a*]indene (**5**) (500 mg, 0.76 mmol) in carbon tetrachloride (25 mL) at room temperature was added $CuBr_2Al_2O_3$ (2.4 g). After 5 h at 80 °C, the reaction mixture was filtered, and the precipitate was washed with carbon tetrachloride (3 × 100 mL). The combined organic extract was concentrated under reduced pressure, and the solid residue was purified by flash chromatography to give 450 mg (73%) of dibromide compound **6** as a white solid: mp 90 °C; R_f 0.85 (SiO_2, 100% hexane); ^{1}H NMR (300 MHz, $CDCl_3$, δ) 0.52−1.04 (m, 60H), 1.94 (d, J = 6.8 Hz, 8H), 7.17 (d, J = 8.0 Hz, 2H), 7.37 (d of d, J = 8.0 and 1.4 Hz, 2H), 7.49 (s, 2H); ^{13}C NMR (75 MHz, $CDCl_3$, δ) 10.34, 13.98, 23.05, 26.82, 27.35, 30.86, 34.11, 34.73, 54.15, 118.31, 120.83, 126.80, 129.37, 139.05, 155.18, 157.75; HRMS (FAB$^+$, m/z) [M]$^+$ calcd for $C_{48}H_{74}{}^{79}Br^{79}Br$ 808.4157, found 808.4156. Anal. Calcd for $C_{48}H_{73}Br_2$: C 71.09, H 9.20. Found: C 70.58, H 9.78.

Synthesis of Poly(5,5,10,10-tetrakis(2-ethylhexyl)-5,10-dihydroindeno[2,1-*a*]indene-2,7-diyl) (PININE). In a three neck flask were placed $Ni(COD)_2$ (446 mg, 1.62 mmol), 2,2′-dipyridyl (256 mg, 1.62 mmol), cyclooctadiene (0.20 mL, 1.62 mmol), and *N,N*-dimethylformamide (DMF) (8 mL). After three freeze−thaw cycles, the catalyst was heated to 80 °C for 30 min to form the purple complex. The reaction mixture was treated with 2,7-dibromo-5,5,10,10-tetrakis(2-ethylhexyl)-5,10-dihydroindeno[2,1-*a*]indene (**6**) (600 mg, 0.74 mmol) in toluene (8 mL), and heated at 80 °C for 4 days. After cooling to room temperature, the reaction mixture was poured into a mixture of 1 N HCl solution (100 mL), acetone (100 mL), and methanol (200 mL), and stirred for 6 h. The precipitate was filtered, redissolved in chloroform and precipitated again with a large amount of methanol. The obtained pale yellow solid was dried in vacuum at 60 °C for 48 h to give 0.30 g (62%) of poly(5,5,10,10-tetrakis(2-ethylhexyl)-5,10-dihydroindeno[2,1-*a*]indene-2,7-diyl) (PININE) as a yellow solid: ^{1}H NMR (300 MHz, $CDCl_3$, δ) 0.59−1.94 (m, 68H), 7.34−7.62 (m, 6H). Anal. Calcd for $C_{48}H_{74}$: C 88.54, H 11.46. Found: C 87.26, H 11.77.

Synthesis of 4,4,5,5-Tetramethyl-2-[5,5,10,10-tetrakis(2-ethylhexyl)-7-(4,4,5,5-tetramethyl-1,3,2-dioxaborolan-2-yl)-4b,5,9b,10-tetrahydroindeno[2,1-*a*]inden-2-y]-1,3,2-dioxaborolane (7). To a stirred solution of dibromo compound **6** (0.5 g, 0.617 mmol) in THF (10 mL) at −78 °C under argon was slowly added *n*-BuLi (1.60 M in hexane) (0.963 mL, 1.54 mmol). After 1 h at −78 °C, the reaction mixture was treated with 2-isopropoxy-4,4,5,5-tetramethyl-1,3,2-dioxaborolane (68 mg, 0.367 mmol). The reaction mixture was stirred for 3 h at room temperature, and treated with 1 N aqueous HCl solution (4 mL). The organic phase was isolated and the aqueous phase was extracted with diethyl ether (2 × 100 mL). The combined organic phase was dried with $MgSO_4$, concentrated under reduced pressure, and purified by flash chromatography to give 478 mg (79%) of compound **8** as a white solid: R_f 0.45 (SiO_2, methylene chloride:hexane = 1:4); ^{1}H NMR (300 MHz, $CDCl_3$, δ) 0.46−1.04 (m, 60H), 1.37(s, 24H), 2.05 (d, J = 9.1 Hz, 8H), 7.32 (d, J = 7.7 Hz, 2H), 7.70 (d of d, J = 7.7 and 0.8 Hz, 2H), 7.81 (s, 2H); ^{13}C NMR (75 MHz, $CDCl_3$, δ) 9.42, 10.51, 14.03, 23.08, 24.81, 26.42, 27.54, 28.26, 34.59, 53.83, 83.37, 119.33, 123.78, 129.08, 133.41, 143.40, 154.79, 157.35; HRMS (FAB$^+$, m/z) [M]$^+$ calcd for $C_{60}H_{98}B_2O_4$ 904.7651, found 904.7653. Anal. Calcd for $C_{60}H_{98}B_2O_4$: C 78.78, H 10.42, B 2.73, O 8.07. Found: C 79.32, H 10.79, O 3.60.

Synthesis of Alternating Copolymers, PININEBT, PININEDTBT, PININEDHTBT, and PININEDHOTBT. Carefully purified 4,4,5,5-tetramethyl-2-[5,5,10,10-tetrakis(2-ethylhexyl)-7-(4,4,5,5-tetramethyl-1,3,2-dioxaborolan-2-yl)-4b,5,9b,10-tetrahydroindeno[2,1-*a*]inden-2-yl]-1,3,2-dioxaborolane (**7**), various monomer (**8**−**11**), and $(PPh_3)_4Pd(0)$ (3 mol%) were dissolved in a mixture of toluene and aqueous 2 M Na_2CO_3. The mixture was refluxed with vigorous stirring for 3 days under argon atmosphere. After the mixture was cooled to room temperature, it was poured into methanol. The resulting solid material was reprecipitated using 50 mL of THF/1.0 L of methanol several times to generate PININEBT (copolymer with benzothiadiazole), PININEDTBT (copolymer with 4,7-di-2-thienyl-2,1,3-benzothiadiazole), PININEDHTBT (copolymer with 4,7-bis(4-hexyl-2-thienyl)-2,1,3-benzothiadiazole), and PININEDHOTBT (copolymer with 4,7-bis[3-(hexyloxy)-2-thienyl]-2,1,3-benzothiadiazole) with the yields of 45 to 67%. The resulting polymers were soluble in THF, $CHCl_3$, *o*-dichlorobenzene and toluene.

Acknowledgment. We thank Prof. Alan J. Heeger of UC Santa Barbara for productive interactions through the GRL Program and for access to equipment used for some of the measurements. This work was supported by the Ministry of Information & Communications, Korea, under the Information Technology Research Center (ITRC) Support Program and International Cooperation Research Program of the Ministry of Science & Technology, Korea (Global Research Laboratory, M6-0605-00-0005).

Supporting Information Available: ^{1}H NMR, ^{13}C NMR and mass spectroscopy of monomers and polymers; thermogravimetric analysis of the PININE; PL spectra of Si-PPV and PFV at the different exposure times; current−voltage characteristics for the solar cells as various ratio of PININEDTBT:PCBM. This material is available free of charge via the Internet at http://pubs.acs.org.

References and Notes

(1) Burroughes, J. H.; Bradley, D. D. C.; Brown, A. R.; Marks, R. N.; Mackay, K.; Friend, R. H.; Burns, P. L.; Holmes, A. B. *Nature* **1990**, *347*, 539.
(2) Dini, D.; Martin, R. E.; Holmes, A. B. *Adv. Funct. Mater.* **2002**, *12*, 299.
(3) Yu, G.; Gao, J.; Hummelen, J. C.; Wudl, F.; Heeger, A. J. *Science* **1995**, *270*, 1789.
(4) Huynh, W. U.; Dittmer, J. J.; Alivisatos, A. P. *Science* **2002**, *295*, 2425.
(5) Xin, H.; Kim, F. S.; Jenekhe, S. A. *J. Am. Chem. Soc.* **2008**, *130*, 5424.
(6) Hsieh, B. R.; Wan, W. C.; Yu, Y.; Cao, Y.; Goodwin, T. E.; Gonzalez, S. A.; Feld, W. A. *Macromolecules* **1998**, *31*, 631.
(7) Gong, X.; Moses, D.; Heeger, A. J.; Liu, S.; Jen, A. K. Y. *Appl. Phys. Lett.* **2003**, *83*, 183.
(8) Lin, Y. Y.; Cheng, C.; Liao, H. H.; Horng, S. F.; Meng, H. F.; Hsu, C. S. *Appl. Phys. Lett.* **2006**, *89*, 063501.
(9) Greenham, N. C.; Moratti, S. C.; Bradley, D. D. C.; Friend, R. H.; Holmes, A. B. *Nature* **1993**, *365*, 628.

(10) Peng, Z. H.; Galvin, M. E. *Chem. Mater.* **1998**, *10*, 1785.
(11) Sun, R. G.; Wang, Y. Z.; Wang, D. K.; Zheng, Q. B.; Kyllo, E. M.; Gustafson, T. L.; Wang, F.; Epstein, A. J. *Synth. Mat* **2000**, *111*−*112*, 595.
(12) Liu, B.; Yu, W. L.; Lai, Y. H.; Huang, W. *Chem. Mater.* **2001**, *13*, 1984.
(13) Guo, T. F.; Pyo, S.; Chang, S. C.; Yang, Y. *Adv. Funct. Mater.* **2001**, *11*, 339.
(14) Suh, H.; Jin, Y.; Park, S. H.; Kim, D.; Kim, J.; Kim, C.; Kim, J. Y.; Lee, K. *Macromolecules* **2005**, *38*, 6285.
(15) Park, S. H.; Jin, Y.; Kim, J. Y.; Kim, S. H.; Kim, J.; Suh, H.; Lee, K. *Adv. Funct. Mater.* **2007**, *17*, 3063.
(16) Zhu, Y.; Gibbons, K. M.; Kulkarni, A. P.; Jenekhe, S. A. *Macromolecules* **2007**, *40*, 804.
(17) Grisorio, R.; Suranna, G. P.; Mastrorilli, P.; Nobile, C. F. *Org. Lett.* **2007**, *9*, 3149.
(18) Shi, C.; Yao, Y.; Yang, Y.; Pei, Q. *J. Am. Chem. Soc.* **2006**, *128*, 8980.
(19) Blouin, N.; Michaud, A.; Gendron, D.; Wakim, S.; Blair, E.; Neagu-Plesu, R.; Belletete, M.; Durocher, G.; Tao, Y.; Leclerc, M. *J. Am. Chem. Soc.* **2008**, *130*, 732.
(20) Pei, Q.; Yang, Y. *J. Am. Chem. Soc.* **1996**, *118*, 7416.
(21) Kreyenschmidt, M.; Klaerner, G.; Fuhrer, T.; Ashenhurst, J.; Karg, S.; Chen, W. D.; Lee, V. Y.; Scott, J. C.; Miller, R. D. *Macromolecules* **1998**, *31*, 1099.
(22) Papadimitrakopoulos, F.; Konstadinidis, K.; Miller, T. M.; Opila, R.; Chandross, E. A.; Galvin, M. E. *Chem. Mater.* **1994**, *6*, 1563.
(23) Zyung, T.; Kim, J. J. *Appl. Phys. Lett.* **1995**, *67*, 3420.
(24) Ke, L.; Chen, P.; Chua, S. J. *Appl. Phys. Lett.* **2002**, *80*, 697.
(25) Rothberg, L. J.; Yan, M.; Son, S.; Galvin, M. E.; Kwock, E. W.; Miller, T. M.; Katz, H. E.; Haddon, R. C.; Papadimitrakopoulos, F. *Synth. Met.* **1996**, *78*, 231.
(26) Cumpston, B. H.; Jensen, K. F. *Synth. Met.* **1995**, *73*, 195.
(27) Hale, G. D.; Oldenburg, S. J.; Halas, N. J. *Appl. Phys. Lett.* **1997**, *71*, 1483.
(28) Scurlock, R. D.; Wang, B.; Ogilby, P. R.; Sheats, J. R.; Clough, R. L. *J. Am. Chem. Soc.* **1995**, *117*, 10194.
(29) Lux, A.; Holmes, A. B.; Cervini, R.; Davies, J. E.; Moratti, S. C.; Grüner, J.; Cacialli, F.; Friend, R. H. *Synth. Mat.* **1997**, *84*, 293.
(30) Oelgemöller, M.; Brem, B.; Frank, R.; Schneider, S.; Lenoir, D.; Hertkorn, N.; Origane, Y.; Lemmen, P.; Lex, J.; Inoue, Y. *J. Chem. Soc., Perkin Trans. 2* **2002**, *2002*, 1760.
(31) Suzuki, N.; Kazui, Y.; Izawa, Y. *Tetrahedron Lett.* **1982**, *23*, 95.
(32) Ma, W.; Yang, C.; Gong, X.; Lee, K.; Heeger, A. J. *Adv. Funct. Mater.* **2005**, *15*, 1617.
(33) Reyes-Reyes, M.; Kim, K.; Carroll, D. L. *Appl. Phys. Lett.* **2005**, *87*, 083506.
(34) Schilinsky, P.; Asawapirom, U.; Scherf, U.; Biele, M.; Brabec, C. J. *Chem. Mater.* **2005**, *17*, 2175.
(35) Li, G.; Shrotriya, V.; Huang, J.; Yao, Y.; Moriarty, T.; Emery, K.; Yang, Y. *Nat. Mater.* **2005**, *4*, 864.
(36) Berlin, A.; Zotti, G.; Zecchin, S.; Schiavon, G.; Vercelli, B.; Zanelli, A. *Chem. Mater.* **2004**, *16*, 3667.
(37) Blondin, P.; Bouchard, J.; Beaupre, S.; Belletete, M.; Durocher, G.; Leclerc, M. *Macromolecules* **2000**, *33*, 5874.
(38) Lévesque, I.; Donat-Bouillud, A.; Tao, Y.; D'Iorio, M.; Beaupré, S.; Blondin, P.; Ranger, M.; Bouchard, J.; Leclerc, M. *Synth. Met.* **2001**, *122*, 79.
(39) Charas, A.; Barbagallo, N.; Morgado, J.; Alcacer, L. *Synth. Met.* **2001**, *122*, 23.
(40) Herguth, P.; Jiang, X.; Liu, M. S.; Jen, A. K. Y. *Macromolecules* **2002**, *35*, 6094.
(41) Brabec, C. J.; Winder, C.; Sariciftci, N. S.; Hummelen, J. C.; Dhanabalan, A.; Hal, P. A.; Janssen, R. A. J. *Adv. Funct. Mater.* **2002**, *12*, 709.
(42) Padinger, F.; Rittberger, R. S.; Sariciftci, N. S. *Adv. Funct. Mater.* **2003**, *13*, 85.
(43) Brabec, C. J. *Sol. Energy Mater. Sol. Cells* **2004**, *83*, 273.
(44) Yang, J.; Jiang, C.; Zhang, Y.; Yang, R.; Yang, W.; Hou, Q.; Cao, Y. *Macromolecules* **2004**, *37*, 1211.
(45) Grell, M.; Donal, D. C.; Bradley, D. D. C.; Inbasekaran, M.; Woo, E. P. *Adv. Mater.* **1997**, *9*, 798.
(46) Leclerc, M. *J. Polym. Sci., Part A: Polym. Chem.* **2001**, *39*, 2867.
(47) Suzuki, H.; Yokoo, A.; Notomi, M. *Polym. Adv. Technol.* **2004**, *15*, 75.
(48) Rao, V. D.; Periasamy, M. *Synthesis* **2000**, *2000*, 703.
(49) Chuen, C. C.; Fenton, S. W. *J. Org. Chem.* **1958**, *23*, 1538.
(50) Yamamoto, T.; Morita, A.; Miyazaki, Y.; Maruyama, T.; Wakayama, H.; Zhou, Z. H.; Nakamura, Y.; Kanbara, T.; Sasaki, S.; Kubota, K. *Macromolecules* **1992**, *25*, 1214.
(51) Burn, P. L.; Holmes, A. B.; Kraft, A.; Bradley, D. D. C.; Brown, A. R.; Friend, R. H.; Gywer, R. W. *Nature* **1992**, *356*, 47.
(52) D'Andrade, B. W.; Holmes, R. J.; Forrest, S. R. *Adv. Mater.* **2004**, *16*, 624.
(53) Waldauf, C.; Shilincky, P.; Hauch, J.; Brabec, C. J. *Thin Solid Films* **2004**, *451*−*452*, 503.

MA801420E